Cellulose (2022) 29:3467–3482
https://doi.org/10.1007/s10570-022-04487-9

ORIGINAL RESEARCH

Ionic liquid regenerated cellulose membrane electroless plated by silver layer for ECG signal monitoring

Xueli Fu · Yanping Wang · Wei Wang · Dan Yu

Received: 13 July 2021 / Accepted: 15 February 2022 / Published online: 7 March 2022

Abstract Nowadays, more and more attention has been paid to flexible electrodes, which can be used to make wearable devices so as to monitor health signals, such as those in ECG, EMG and EEG. However, the contact impedance of many membrane electrodes is high due to the bad fit between the sensors and the skin, or the poor sensitivity caused by low conductivity. Therefore, we fabricated a skin-like conductive electrode via electroless silver plating on the surface of regenerated cellulose membrane, which was prepared from the cellulose dissolved in ionic liquid [Bmim]Cl. The as-prepared biocompatible electrodes with low skin-electrode contact impedance can be used as a dry electrode for a long time. Its impedance at 700 Hz is only 8 kΩ/cm^2 and the conductivity reaches 252 s/cm. After 5 h of wearing, the electrode-skin contact impedance at 700 Hz is only 10 kΩ/cm^2 when 0.20 mol/L $AgNO_3$ is used. In short, the prepared electrode can not only ensure stable and clear ECG signals but also can greatly reduce electrode–skin contact impedance when used for long-term health monitoring.

X. Fu · Y. Wang · W. Wang · D. Yu (✉)
Key Laboratory of Science and Technology of Eco-Textile, College of Chemistry, Chemical Engineering and Biotechnology, Donghua University, Ministry of Education, 2999 North Renmin Road, Songjiang District, Shanghai 201620, China
e-mail: yudan@dhu.edu.cn

Graphical abstract

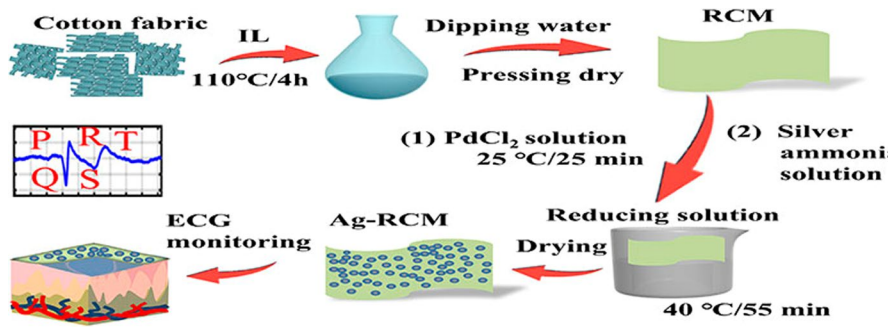

Keywords [Bmim]Cl · Recycled cellulose membrane · Electroless plating · Flexible electrodes · ECG

Introduction

Currently, the electrocardiograph (ECG), electromyogram (EMG) and electroencephalogram (EEG) sensors are widely used in personal healthcare and hospitals to monitor human heart activity (Lam et al. 2020; Tan et al. 2011; Yoon et al. 2009). The electrodes are the most important components in ECG monitoring devices and are usually classified as either "wet" or "dry", depending on the use of electrolytes or not. At present, Ag/AgCl electrode, a commercial wet electrode, is commonly used, but it is not suitable for long-term use with high cost. The skin feels uncomfortable under Ag/AgCl electrode and its conductive gel easily gets dried over time. Therefore, the exploration of dry electrodes is persistently carried out. Researches mainly focused on the dry electrodes made of membrane, microneedle electrodes and fabric, such as cotton fabric, polyester fabric and conductive wires, which are, however, usually heavy and uncomfortable (Nigusse et al. 2020; Xu et al. 2019; Zhou et al. 2014). So it is important to develop a well-adapted new type of electrode for ECG signal monitoring.

Besides good sensitivity, low impedance of the electrode is also important. The acquisition impedance always increases when there is a gap between the electrodes and the skin, which results in poor ECG quality and reduces the accuracy of monitoring (Beckmann et al. 2010; Catrysse et al. 2004). To address this problem, many researches have been done. Electrodes were designed based on polydimethylsiloxane (PDMS), polyethylene terephthalate (Zhao et al. 2008) and polyimide so as to reduce the skin-electrode contact impedance. By preparing Multi-walled carbon nanotube (MWCNT)/PDMS complexes and combining them with Kapton substrates (Tasneem et al. 2020) created flexible and biocompatible electrodes with low skin-electrode contact impedance. Liu et al. (2020) created a flexible and stretchable three-layer dry electrode with excellent conformability and stretchability, as well as low electrode-skin contact impedance, using transfer printing. Despite their advantages, the conductive materials like MWCNTs are not evenly dispersed in PDMS or TPU, which inevitably affects the conductivity of the dry electrode. In this experiment, electroless plating, rather than other metalizing methods like coating, printing, plasma plating or magnetron sputtering, was used to endow the substrates with good electrical conductivity. Electroless plating is essentially a redox reaction to metal ions and can be easily conducted without using any expensive instrument.

Many methods can be used to deposit metals on substrates, such as electroless plating, coating and magnetron sputtering (Jin et al. 2017; Pan et al. 2017). In electroless plating, metal ions are reduced to simple substances and deposited onto the surface of the substrate, using a reducing agent. Sarafpour et al. (2017) coated polypropylene fabrics with copper particles using electroless plating, screen printing and arc spraying process. The tensile strength, electrical conductivity, air permeability, thermal conductivity and fog collection capacity of electroless

copper plated fabrics are higher than those of screen printed and sprayed copper-coated fabrics. Magnetron sputtering, also known as plasma plating, mainly involves the deposition of atoms to the target material using ions with high energy. Wu et al. (2019) fabricated a flexible wearable pressure sensor by magnetron sputtering. The coating method is used to prepare conductive fabrics by applying coatings containing conductive fillers (e.g., metal powders) to fabrics. Nigusse (2020) coated cotton and polyester fabrics with silver ink by screen printing, so as to monitor ECG signals. However, after being coated, the substrates are always stiff and cannot be fixed on human body or joints comfortably. Besides, magnetron sputtering is not commonly used due to its high price. Therefore, it is important to develop biocompatible electrodes with low skin-electrode contact impedance in an expedient and environmentally friendly way.

There are many dissolution systems for cellulose, including N-methyl morpholine-N-oxide (NMMO), alkaline aqueous dissolution system, ionic liquids and LiCl/DMAc (N, N-di-methylacetamide). NMMO can dissolve cellulose effectively (Zhao et al. 2007). However, its prices are high and dissolution conditions are harsh. It is also hard to control its reaction by-products (Rosenau and French 2021). As for LiCl/DMAc, it does not result in any thermal runaway reaction and no additives or special equipment are needed. It can also be recycled. But LiCl is expensive (Huber et al. 2011). In contrast, as a type of green solvent, ionic liquids are not only recyclable and environmentally friendly, but also have a good thermal and chemical stability. Ma et al. (2016) prepared cellulose membranes using [Bmim]Cl, which has good thermal stability and high moisture regain. Ionic liquids were used to prepare ionic gels with properties of ECG sensors. Jo et al. (2020) prepared biodegradable and solid electrolyte-based organic transistors based on levoglycans and choline-based ionic liquids, and then prepared ionic gels for ECG signal monitoring. In addition, the high biocompatibility and flexibility of cellulose membranes make them flexible base materials.

Therefore, in this paper, an electrically conductive electrode with low skin–electrode contact impedance was fabricated by electroless silver plating on a regenerated cellulose film (RCM). The RCM was prepared by dissolving cotton fibers in ionic liquids. It is environmentally friendly and requires no excessive reagents. Besides, electroless plating is simple and effective for metal deposition. The resultant electrodes were characterized by FTIR, thermal stability, field emission scanning electron microscopy, XPS and XRD. Furthermore, the electrochemical properties and ECG monitoring properties of the electrodes were also tested.

Experiment

Materials

In this experiment, the 200*200 cm^2 cotton fabric was bought from Shanghai San yuan Co. Ltd. [Bmim]Cl (97% purity) was supplied by Shanghai Bidder Medical Technology Co. Ltd. Glucose (> 99% purity), potassium sodium tartrate (> 99% purity), palladium chloride (AR), anhydrous ethanol, and ethylenediamine (> 99.8% purity) were obtained from Sinopharm Chemical Reagent Co. Ltd. Ammonia (25 ~ 28 purity) was obtained from Beijing Yinuo Technology Co., Ltd. Potassium hydroxide (> 85% purity) was obtained from Shanghai Lingfeng Chemical Reagent Co. Ltd. Silver nitrate (> 99.8% purity) was purchased from Shanghai Titan Technology Co. Ltd.

All chemicals are analytical grade reagents and used without purification.

Preparation of RCM

RCM was prepared using [Bmim]Cl. [Bmim]Cl (4 g) was put into a round bottom flask in an oil bath at 110 °C. When its color turned into transparent yellow, cotton fiber (0.20 g) was added to the flask. The compound was stirred mechanically until [Bmim]Cl was completely dissolved with cotton fiber (when no cotton fibers could be observed through the microscope). Then, the solution was kept in the flask at 110 °C for 30 min to remove bubbles. The solution was next poured into the mold and was cooled to room temperature to obtain a cellulose hydrogel, which was further soaked in water for 5 days to completely remove [Bmim]Cl. Finally, a transparent

regenerated cellulose membrane (RCM) was obtained after natural drying.

Preparation of Ag-RCM

Ag-RCM was prepared by electroless plating. First, glucose (2 g), potassium sodium tartrate (0.125 g), and polyethylene glycol (0.003 g) were weighed and dissolved in 50 ml of distilled water to prepare the reducing solution, to which ethanol (2 ml) was then added. The compound was next shaken to be mixed well. Second, to prepare silver ammonia solution, $AgNO_3$ (0.05, 0.01, 0.15, 0.20 mol) was weighed and dissolved in 12.5 ml of distilled water. And ammonia was added to it dropwise until the solution just became clarified. Then the solution obtained from 0.3 g KOH dissolved in 2.5 ml of distilled water was added to it to get a dark brown solution. Next, ammonia was added dropwise to clarify the solution. After adding 2 ml of ethylenediamine, the solution was shaken well. Third, the RCM and the silver ammonia solution were put into the reducing solution to be sonicated at 40 °C for 55 min. Finally, after being rinsed with deionized water, Ag-RCM was obtained.

Characterization

FTIR spectrum Fourier transform infrared (FTIR) spectra

The FTIR spectra of Cellulose and RCM were obtained with a Fourier infrared spectrometer (FTIR, Nicolet 6700, USA) at frequencies of 500–4000 cm^{-1}.

Thermal stability

Thermal stability curves of cellulose, RCM, Ag-RCM were obtained with a thermogravimetric analyzer (TGA, Netzsch, 209 F1, Germany) under a N_2 atmosphere at 0–900 °C with a heating rate of 10 °C/min.

Field emission scanning electron microscope

The morphology of cellulose and Ag-RCM were characterized by a field emission scanning electron microscopy. Before testing, the samples were dried and then gold plated with a vacuum sputtering coater.

XPS spectra

The surface elemental composition and atomic valence state of Ag-RCM in the range of 0 ~ 1200 eV was measured by an X-ray photoelectron spectroscopy (XPS, Escalab 250Xi).

Scanning electron microscope

The structure of the thin silver layer on the cellulose film substrate was analyzed by an 18 KW rotary target X-ray diffractometer (D/max-2550VB + /PC).

Conductivity testing

Electrical properties were measured using a four-point probe surface resistance tester (MCP-T370, Loresta, Japan). The average values of 5 different measurements were selected for the final results and the conductivity was calculated using the formula (1).

$$\delta = 1/R_S * d \quad (1)$$

In Eq. 1, Rs refers to the sheet resistance of the film and d refers to the thickness of the film.

Electrical performance evaluation

The impedance, EIS and open-circuit voltage performance of the electrodes were tested using an electrochemical analyzer (CHI 660E, Chen Hua, China). Impedance and EIS was measured within the frequency range of 0.01 Hz to 100 kHz. The tracking time of the open circuit voltage was 30 s, with a sampling interval of 0.1 s and a potential of −1 to 1 V.

Electrode stability tests

A Date physics TUB 90E goniometer was used to measure the water contact angle (WCA) so as to evaluate the hydrophobic property of the Ag/AgCl electrode, which was also worn on the arm for 5 h to

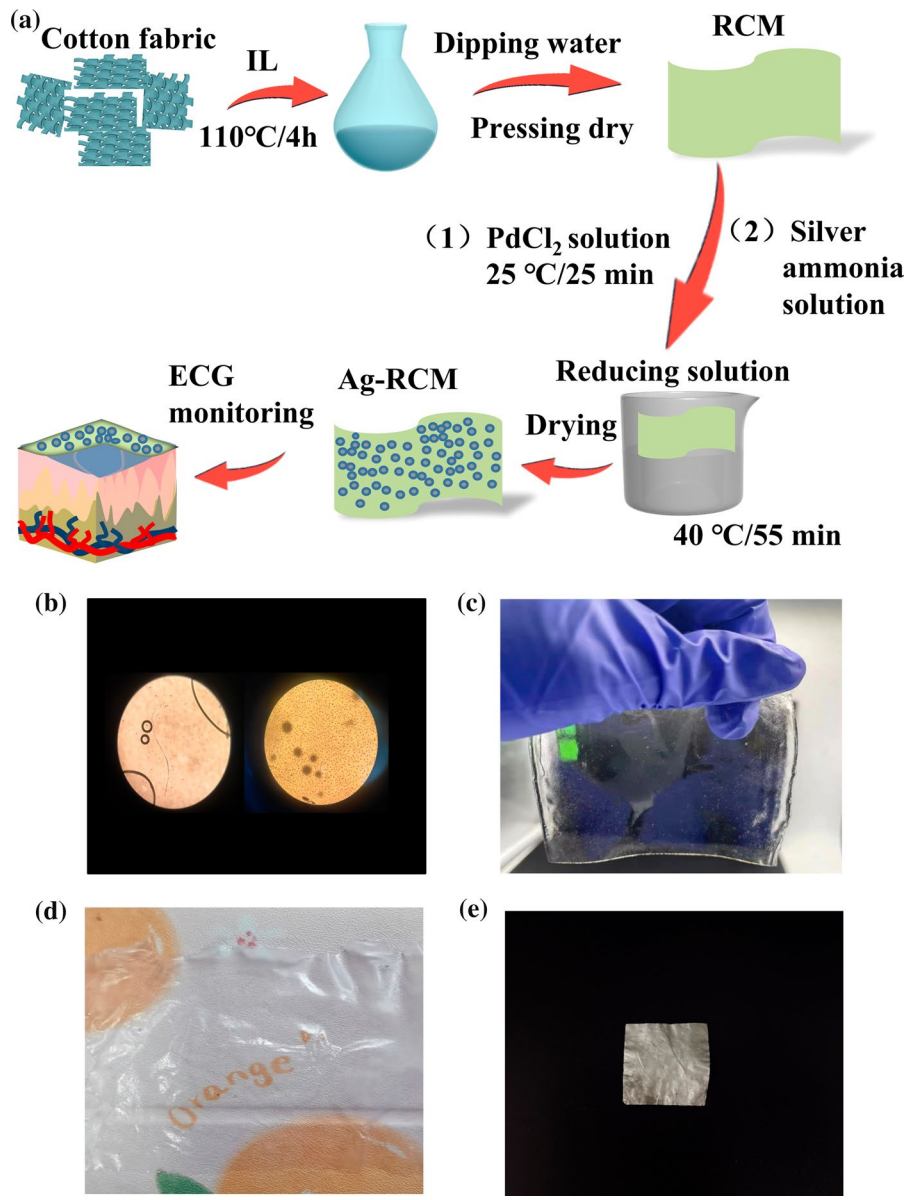

Fig. 1 **a** Schematic diagram of the preparation process of RCM. **b** Cellulose dissolution before and after being magnified 100 times under an optical microscope. **c** Cellulose hydrogel. **d** RCM. **e** Ag-RCM

test its safety. Besides, it was washed in water three times, two minutes each time to test its stability.

ECG tests

The Ag-RCM electrodes were used in the commercial ECG device (BDM101) to test the ECG signals of the volunteers. The digital signals were transmitted to the PC via bluetooth and processed with Matlab2018.

Results and discussion

Design and synthesis process of Ag-RCM

Figure 1a shows the design and preparation process of the Ag-RCM. Cellulose was dissolved with [Bmim]Cl to prepare for RCM. Then the dried RSMs were prepared for Ag-RCM composite conductive films by electroless plating. First, the cotton fibres were added to the melted [Bmim]Cl. Cl^- in [Bmim]Cl, together with H on hydroxyl groups in the cellulose

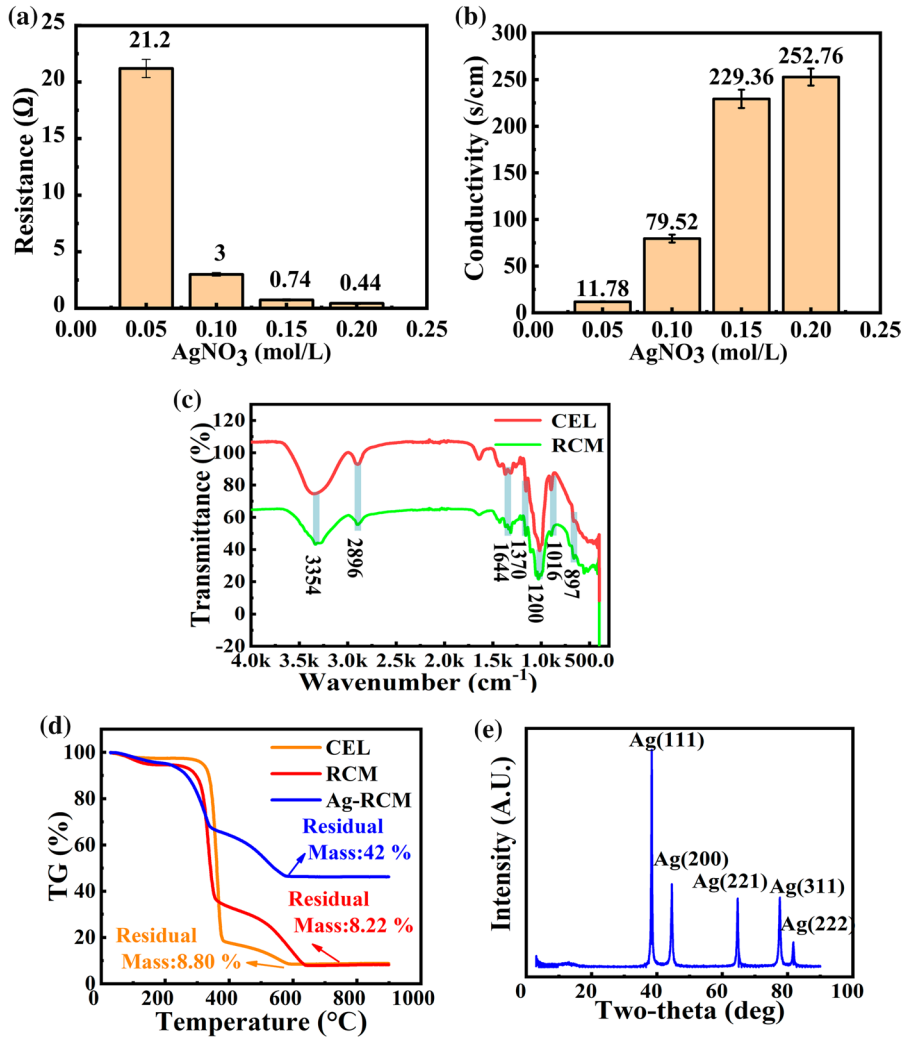

Fig. 2 **a** Resistance of Ag-RCM electrodes. **b** Conductivity of Ag-RCM electrodes. **c** FTIR spectra of CEL and RCM. **d** Thermogravimetric curves of CEL, RCM and Ag-RCM **e** XRD pattern of thin silver layers.

macromolecular chain formed hydrogen bonds, thus breaking a large number of existing hydrogen bonds in the cellulose macromolecular chain. The imidazole cation formed hydrogen bonds with the less spatially restricted cellulose-based oxygen atoms via the aromatic hydrogen, ultimately leading to the dissolution of the cellulose (Ding et al. 2012). Therefore, at the beginning of dissolution, numerous fibers could be seen with the optical microscope. But over time, no fibers could be observed when the cotton fibers were completely dissolved (Fig. 1b). The regenerated cellulose hydrogels were obtained by replacing [Bmim]Cl with distilled water (Ma et al. 2017) (Fig. 1c), since there was a competition between water and [Bmim]Cl when they formed hydrogen bonds with hydroxyl groups on the cellulose (Sun et al. 2009). In this way, the ionic liquid was replaced, and the regenerated cellulose hydrogel was formed. Next, the regenerated cellulose hydrogel was wrapped in absorbent paper and pressed with a heavy weight for 24 h to obtain a flat and transparent RCM (Fig. 1d). After the RCM was added to the palladium chloride solution, the activation process was complete due to the coordination or electrostatic attraction between the –OH and the palladium chloride ions (Pei et al. 2021). The presence of polar hydroxyl groups in the RCM results in a negatively charged surface. When the RCM was placed in a silver ammonia solution, Ag $(NH_3)_2^+$ could be adsorbed on the surface of the RCM due to electrostatic interactions between the polar hydroxyl groups in the cellulose and the electron-rich ether oxygen atoms. Thus, the Ag^+ dissociated from Ag

$(NH_3)_2^+$ formed coordination bonds with the ether-based oxygen atoms. A portion of the Ag^+ on the surface of the RCM was reduced by hydroxyl groups in the cellulose and the remainder was reduced by the glucose solution. Since the reduction potential of palladium ion is lower than that of silver ion, palladium ion was first reduced to palladium particles, which catalyzed the reduction of Ag^+ (Ye et al. 2007). Finally, the flexible Ag-RCM was obtained after electroless plating, as shown in Fig. 1e.

Chemical structure and morphology of the composite films

ECG signals can be collected by converting ionic currents in the organism into electronic currents, which are useful for analysing human health conditions. Besides, the resistance and conductivity of the electrodes, which can reduce the effectiveness of monitoring the ECG signal, must be tested. The results are shown in Fig. 2. As the concentration of $AgNO_3$ increases, the resistance of Ag-RCM gradually decreases from 21.6 to 0.44Ω (Fig. 2a), and its conductivity gradually increases from 11.57 to 252.53 s/cm (Fig. 2b).

FTIR spectra of cellulose (CEL), RCM and Ag-RCM samples were obtained using an FTIR system (FTIR, Nicolet 6700, USA) in the frequency range of 500–4000 cm-1. The results are shown in Fig. 2c. As can be seen, the spectra of RCM and CEL are essentially identical, with no new functional groups being produced and no functional groups disappearing. In the spectrogram, only the intensity and wave number are different, suggesting that there are only physical changes in the dissolution of cellulose by [Bmim]Cl (Yu et al. 2018). This further proves that [Bmim]Cl can dissolve cellulose directly. The absorption peaks at 3354, 2900 and 1060 cm^{-1} correspond to the stretching vibration peaks of –OH, $–CH_2$ and C–O–Cin the cellulose molecule respectively (Johar et al. 2012; Kuo and Lee 2009; Oh et al. 2005), as seen in the Fig. 2c. The vibrational peak at 3354 cm^{-1} belongs to –OH on cellulose, which weakens and moves to a lower wave number after being dissolved by [Bmim]Cl, suggesting that the hydrogen bond is weakened to some extent (Yu et al. 2018). The anions and cations of [Bmim]Cl interacted with cellulose separately during the dissolution of cellulose, which resulted in the weakening of the interaction of hydroxyl groups between the cellulose

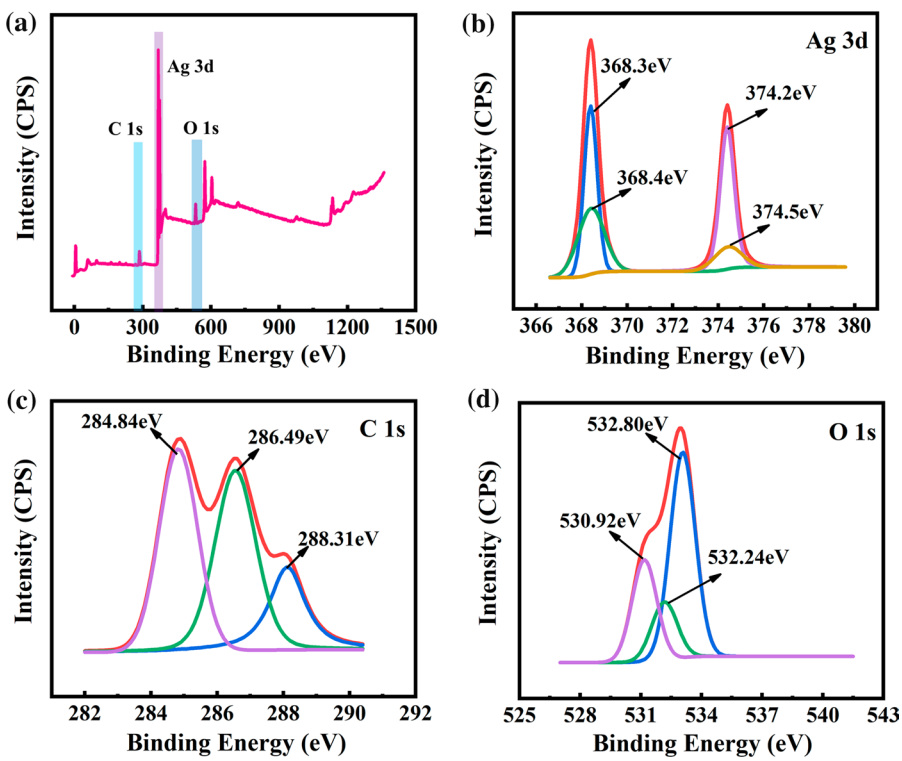

Fig. 3 **a** XPS survey spectra of Ag-RCM. **b–d** XPS spectra of Ag 3d, C 1 s, and O 1 s of Ag-RCM

macromolecular chains. Cellulose recrystallised during the formation of hydrogen bond and its crystallinity decreased.

The thermal stability curves of CEL, RCM and Ag-RCM were obtained by a thermal stability analyzer, which are shown in Fig. 2d. Comparing the thermal stability curves of CEL and RCM, it can be found that both of them have only three stages of thermal decomposition process, and the thermal stability of CEL is better. The residual mass of CEL is 8.98% and that of RCM is 8.22% (899.6 °C). The final residual mass of Ag-RCM is 46.22% (899.6 °C). Therefore, it can be roughly deduced that the mass ratio of Ag is about 36%. From the above data, it can be drawn that the thermal stability of cellulose decreases after being regenerated by [Bmim]Cl. The decrease in the thermal stability of RCM may be caused by the breakage of some hydrogen bonds of cellulose macromolecule chains during the dissolution. Ag-RCM starts decomposition at about 274.1 °C, loses the maximum weight at 513.2℃ and ends the decomposition at 602 °C, during which the silver, with its good thermal conductivity, may accelerate the decomposition (Yao et al. 2016).

Figure 2e shows the XRD spectra of the thin silver layer on the RCM. It can be seen that the positions of the diffraction peaks at 2θ = 38.16°, 44.28°, 64.42°, 77.47°, and 81.53° are consistent with JCPDS card 04–04-0783, corresponding to the (111), (200), (221), (311), and (222) planes, respectively (Chen et al. 2017; Jayram et al. 2016; Todorov et al. 2017). These peaks correspond to the face-centered cubic structure of Ag.

The presence of Ag 3d, C 1 s and O 1 s signals can be clearly seen on the XPS investigation spectra of Ag-RCM (Fig. 3a), which further proves that Ag is deposited on the surface of RCM and oxidized by the air. Figure 3b is the signal spectrum of Ag. If the element loses electrons, the inner electron binding energy will be higher. The binding energy of Ag (3d3/2) shifts from 374.2 to374.4 eV, indicating that Ag loses electrons. Since Ag has only one valence state, it is oxidized by the air. The binding energy of Ag (3d5/2) is 368.3 eV, suggesting the presence of silver on the surface of Ag-RCM. Although the silver may be oxidized, the ligand will not affect it greatly with its low binding energy shift. So the surface of Ag-RCM mainly exists as silver. From Fig. 3c, it can be seen that the surface of Ag-RCM film contains C–H and C–O bonds, whose binding energies are 284.84 and 286.49 eV respectively. The highest binding energy at 288.31 eV belongs to C in CO_3^{2-}, which is due to the formation of the corrosion product Ag_2CO_3 on the surface of the silver. In Fig. 3d, the lowest binding energy at 530.92 eV most likely belongs to Ag_2O. The vibrational peaks at 532.24 and 532.80 eV belong to O in CO_3^{2-}, which is most likely to produce Ag_2CO_3.

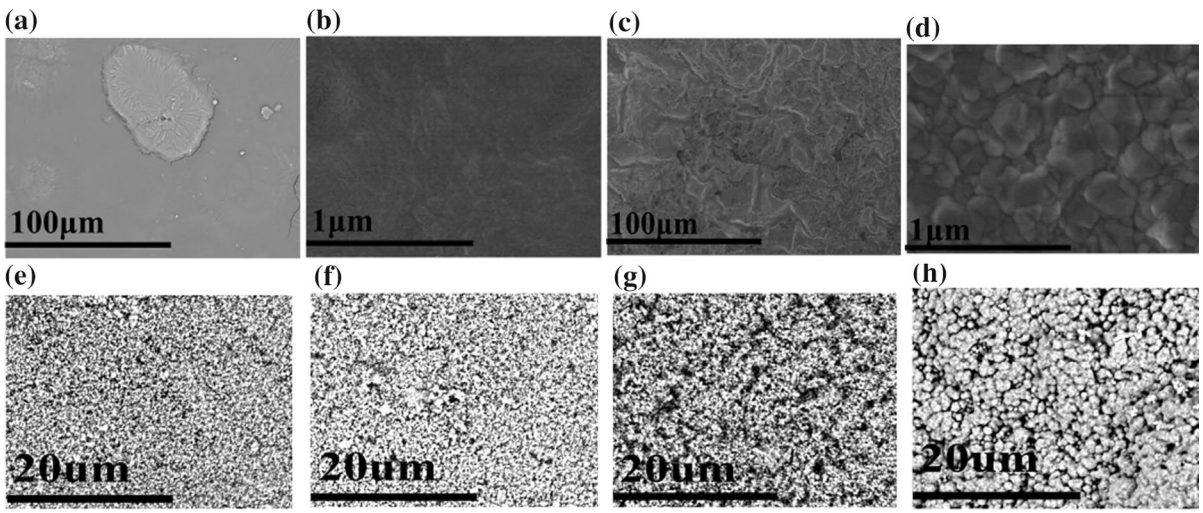

Fig. 4 **a**–**h** SEM images of the films. **a** RCM at low resolution. **b** RCM at high resolution. **c** Ag-RCM at low resolution. **d** Ag-RCM at high resolution. **e**–**h** Particle size of Ag-RCM at the same resolution

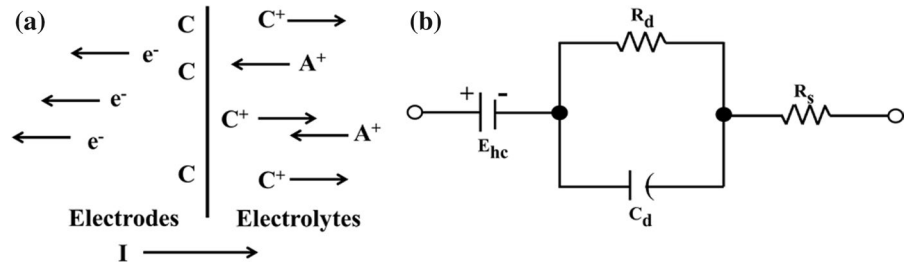

Fig. 5 **a** Ion exchange at the electrode -skin (electrolyte) interface. **b** Electrical equivalent circuit model of the electrode–electrolyte interface

The morphologies of RCM and Ag-RCM were observed by a field emission scanning electron microscope as shown in Fig. 4. The surface of RCM is very flat at low resolution (Fig. 4a), but it is still rough at high resolution (Fig. 4b), which may be due to the loss of moisture during the press-drying process (Kato et al. 2019) or the effect of surface tension (Alawiye et al. 2019). It is also possible that the faster exchange

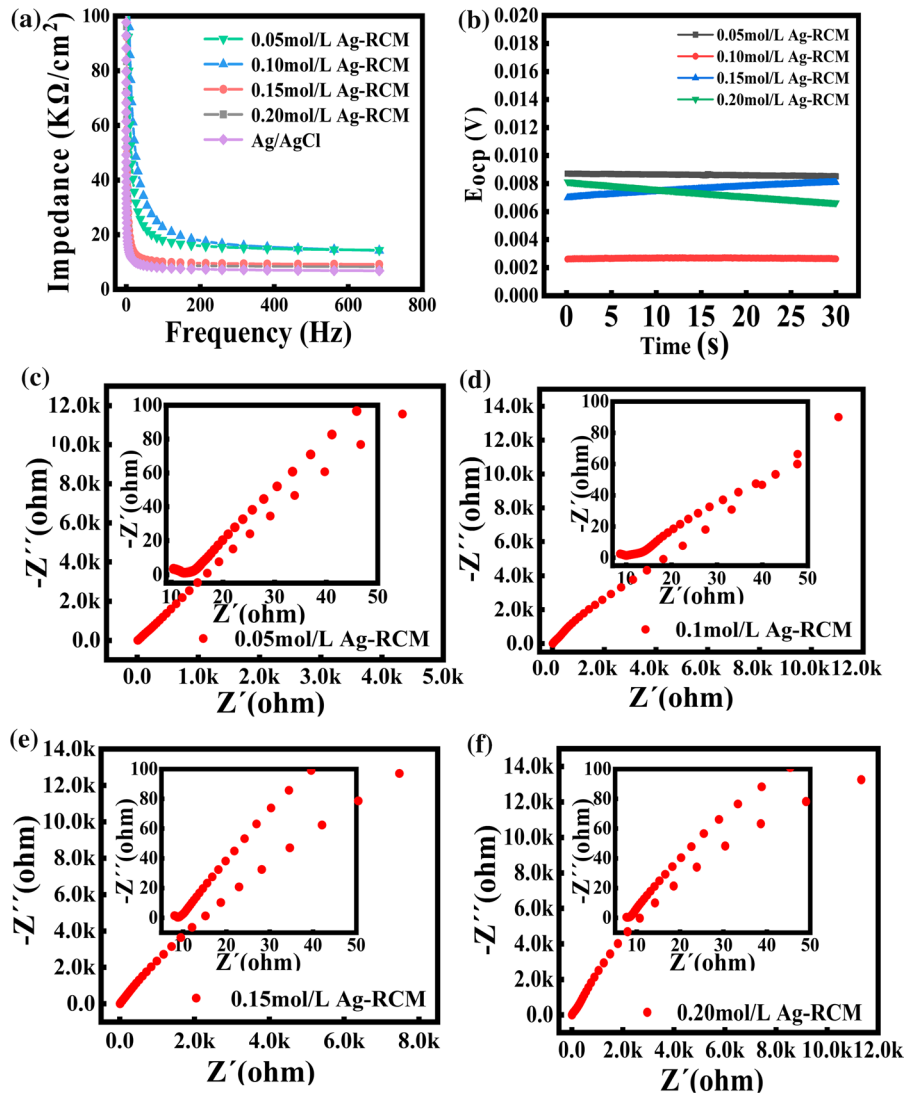

Fig. 6 **a** The skin–electrode contact impedance of the Ag-RCM electrodes and Ag/AgCl electrode. **b** Open circuit voltage of Ag-RCM electrodes. **c**–**f** Nyquist plot of 0.05, 0.10, 0.15 and 0.20 mol/L Ag-RCM electrodes (The inset shows an enlarged view of the high-frequency region)

rate of deionized water and [Bmim]Cl causes wrinkles on the surface of the RCM membrane. After electroless plating, the silver particles were homogeneously deposited on the surface of RCM. The surface of Ag-RCM is rough and dense (Fig. 4c ~ d), for the deposition of silver particles makes the original rough structure more obvious. Numerous pore structures can be observed at high resolution (Fig. 4e ~ h), which is caused by the agglomeration of silver particles (Mackus et al. 2016). The porosity of the surface of Ag-RCM gradually decreases when more and more $AgNO_3$ is added. The pores on the surface of 0.05 mol/L Ag-RCM are smaller and denser than those on the surface of 0.20 mol/L Ag-RCM.

Electrical performance tests of Ag-RCM electrodes

The generation of electrical signals is due to the difference in ion concentrations inside and outside the cell membrane, which is caused by the opening of the ion channels on the cell membrane when the cardiomyocyte receives stimulation. The ECG signals are transmitted to the body surface through human tissues, sensed by electrodes and processed by signal acquisition circuits. The electrodes play a key role in the acquisition of ECG signals, the basic principle being the exchange of ions and electrons. The ions in the electrode material are dissociated into the electrolyte, while the electrons are left in the metal. This process is reversible and the electrochemical reaction equations are shown in Eqs. (2) and (3). The electrical properties of this electrochemical interface can be represented by a classical electrochemical equivalent circuit, as shown in Fig. 5b. The AC impedance of the electrode–electrolyte interface can be expressed in Eq. (4).

$$C \leftrightarrow C^{n+} + ne^{-} \tag{2}$$

$$A^{m-} \leftrightarrow A + me^{-} \tag{3}$$

$$|z| = R_S + \frac{R_d}{1 + j\omega C_d}\omega = 2\pi f \tag{4}$$

In Eq. (4), ω refers to the angular frequency and f refers to the frequency. From Fig. 5b and Eq. (4), it can be seen that at high frequencies, the impedance of the equivalent circuit is $|z| = R_s$, while at low frequencies, the impedance can be expressed as $|z| = Rs + Rd$ when Cd is in an open circuit. The impedance decreases with the increase of frequency over the entire frequency range.

Figure 6 shows the impedance spectra, EIS and open-circuit voltages of Ag-RCM electrodes and commercial Ag/AgCl electrode, monitored by an electrochemical workstation. After a long term wear of the electrode, sweat accumulates between the electrode and the skin, which acts as an electrolyte. So the 20 g/L NaCl and 1 g/L urea solution was used as the simulated sweat solution for skin–electrode impedance testing (Wang et al. 2021). A 1.2×1.0 cm^2 Ag-RCM was used as the working electrode. A large platinum screen was used as the counter electrode and a glycerol electrode was used as the reference electrode. The electrochemical impedance spectrum was scanned at 10 mv, with a scanning frequency of 0.01–1000 Hz. As seen in Fig. 6a, the skin–electrode contact impedance curves of the Ag-RCM electrodes are similar with that of the commercial electrode, for the skin-electrode contact impedance is mainly determined by the skin rather than the electrodes when the skin forms a conformal contact with the electrodes (Liu et al. 2020). The skin–electrode contact impedance curves of 0.15 mol/L Ag-RCM and 0.20 mol/L Ag-RCM largely overlap with that of the commercial electrode, with only about 8 kΩ/cm^2 at 700 Hz. The skin-electrode contact impedances of 0.05 mol/L Ag-RCM and 0.1 mol/L Ag-RCM are slightly higher, but they only reach 18 kΩ/cm^2 at 700 Hz. Therefore, the as-prepared Ag-RCM electrode can be used as an excellent substitute for Ag/AgCl electrodes to monitor ECG signals. Meanwhile, the open-circuit voltage of the Ag-RCM electrode, which can affect the accuracy of the results, must be tested. The scanning of open circuit voltage has a tracking time of 30 s, a sampling interval of 0.1 s and a potential of −1 to 1 V. From Fig. 6b, it can be seen that the open-circuit voltages of all electrodes are relatively stable over time and only fluctuate within a small range. The open-circuit voltages of the 0.05 mol/L Ag-RCM and 0.10 mol/L Ag-RCM electrodes barely fluctuate, while that of the 0.15 mol/L Ag-RCM electrode fluctuate between 0.07 mv and 0.081 mv, and that of the 0.20 mol/L Ag-RCM electrode fluctuate between 0.06 mv ~ 0.08 mv. Therefore, the open-circuit voltage has little effect on the detection of ECG signals.

EIS was used to analyze the electron transport and diffusion of the electrodes. The open-circuit voltage of each electrode was first measured, and then the EIS

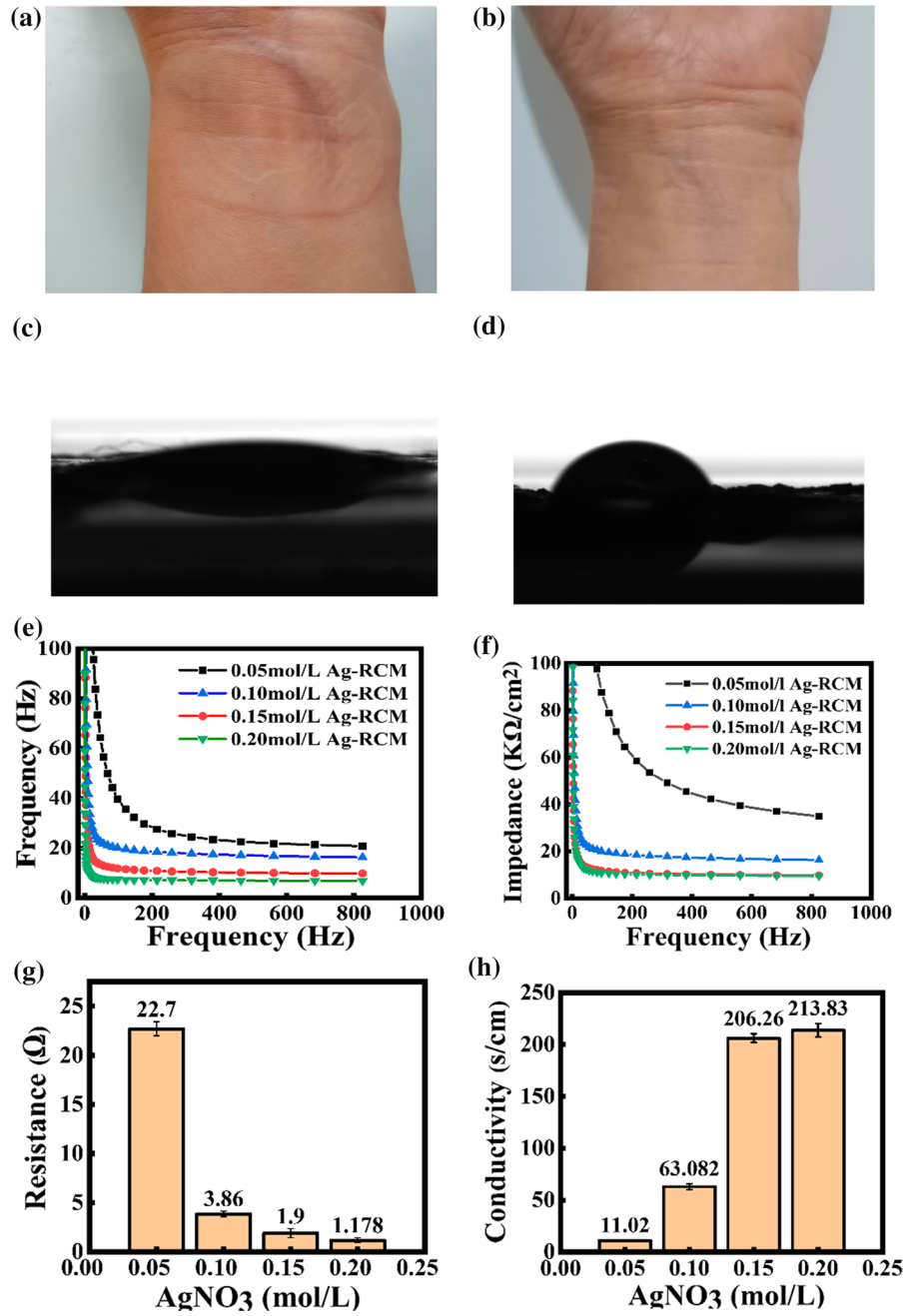

Fig. 7 **a** Photograph of the wrist after wearing the Ag/AgCl electrode for five hours. **b** Photograph of the wrist after wearing the Ag-RCM electrode for five hours. **c** Contact angle of RCM. **d** Contact angle of Ag-RCM. **e** Impedance of Ag-RCM electrode after 5 h of wear. **f** Impedance of Ag-RCM electrode after being washed.**g** Resistance of Ag-RCM electrodes after being bent 100 times. **h** Conductivity of Ag-RCM electrodes after being bent 100 times

test was performed by setting the scanning frequency from 0.01 to 1000 Hz. The results are presented as Nyquist plots, where the Nyquist curves of all Ag-RCMs are almost straight lines (Fig. 6c ~ f), even in the high-frequency region. As the concentration of the $AgNO_3$ increases, the slope of the Nyquist curve gradually increases, indicating a faster ion diffusion at the electrode–electrolyte interface.

Stability tests of Ag-RCM electrode

The stability of the electrodes is also important for the long-term monitoring of ECG signals. The Ag-RCM electrode is hydrophobic due to its dense surface structure (Fig. 7d), which is conducive to its long-term preservation.

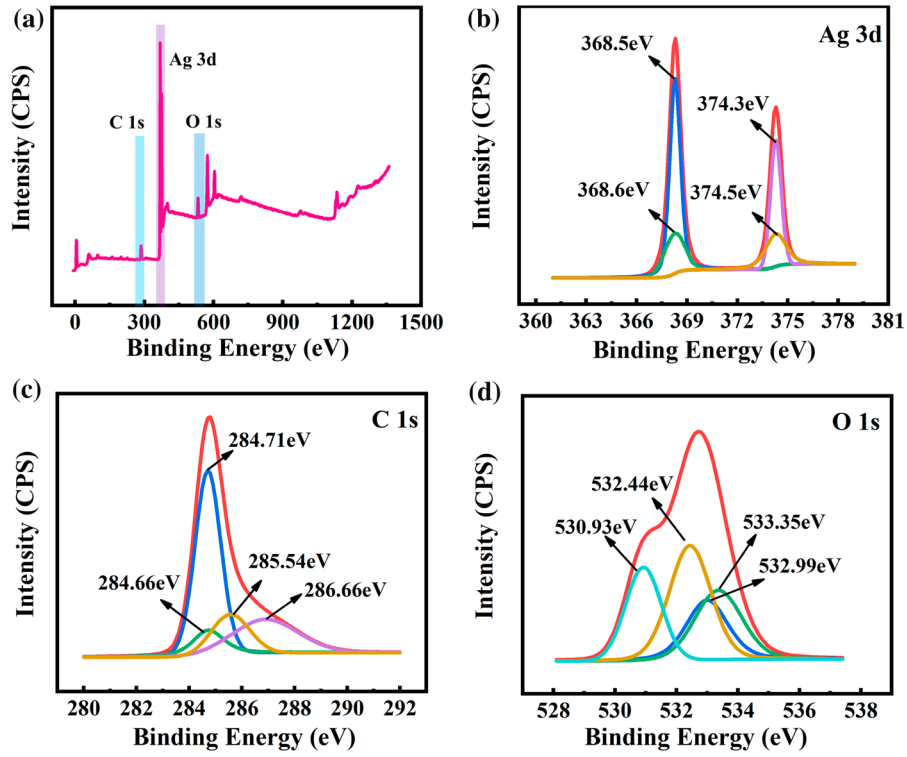

Fig. 8 **a** XPS survey spectra of Ag-RCM after being washed. **b–d** XPS spectra of Ag 3d, C 1 s, and O 1 s of Ag-RCM after being washed

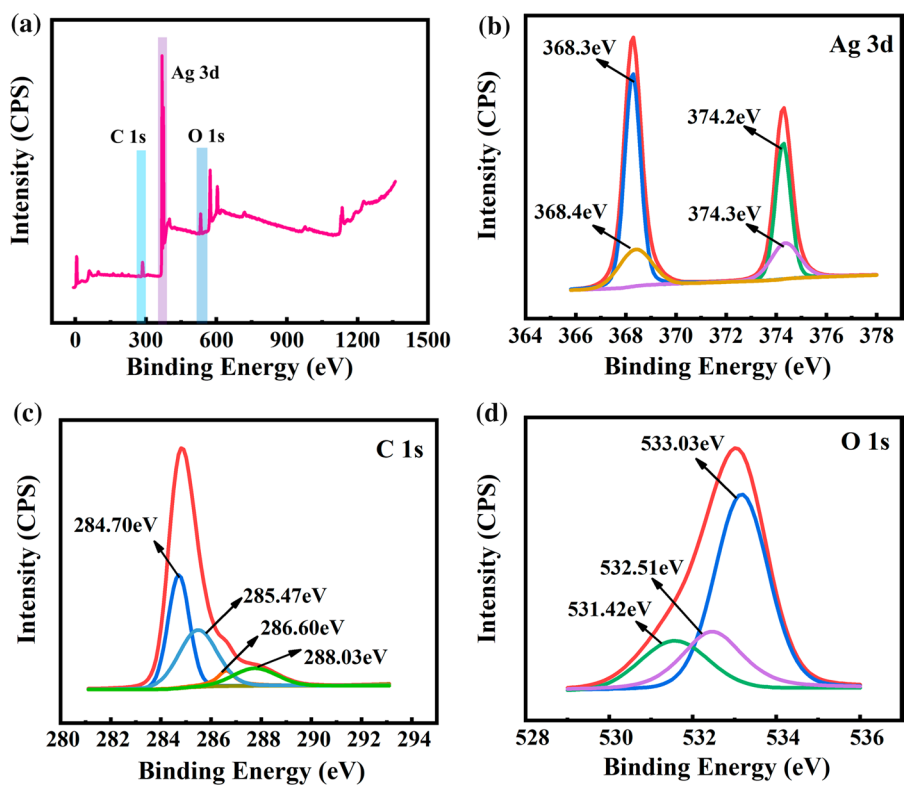

Fig. 9 **a** XPS survey spectra of Ag-RCM after 5 h of wear. **b–d** XPS spectra of Ag 3d, C 1 s, and O 1 s of Ag-RCM after 5 h of wear

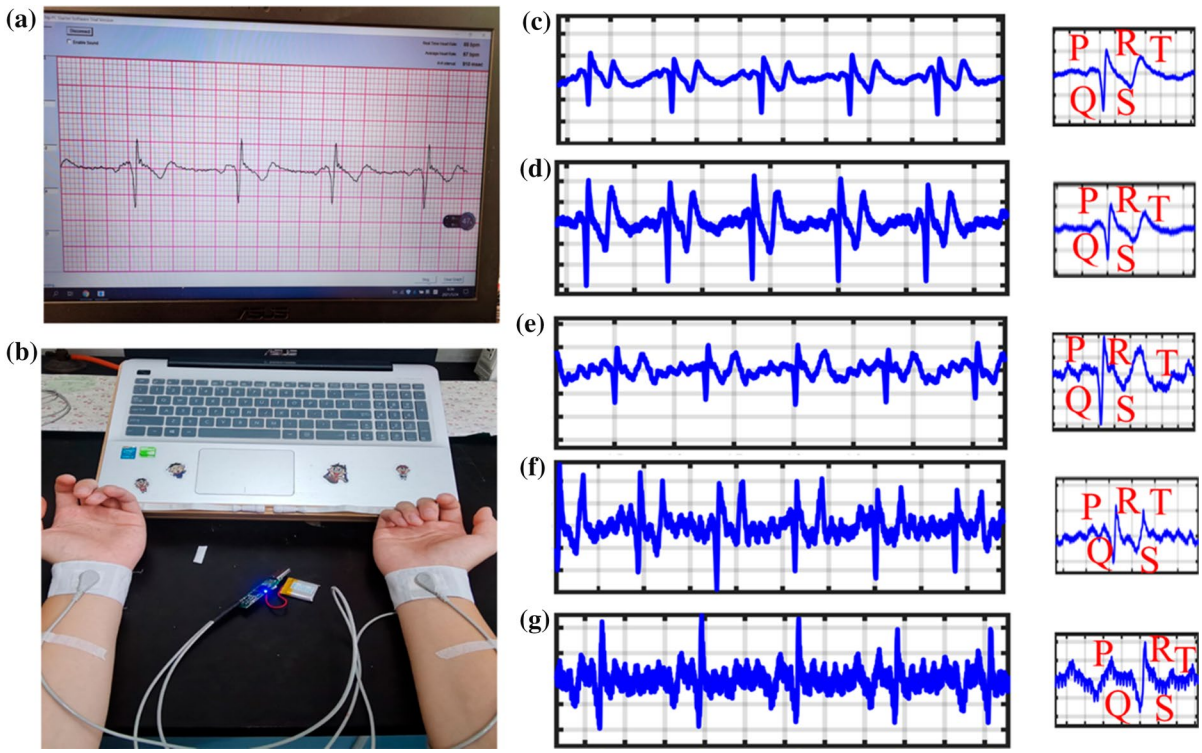

Fig. 10 **a** Picture of the real time ECG signal curve monitored by the pc software. **b** Photographs of the 0.05 mol/L Ag-RCM electrode and the analog front-end circuit. **c**–**g** ECG profiles obtained from 0.05 to 0.20 mol/L Ag-RCM electrode

For a longer period of ECG monitoring, the comfort and safety of the contact between skin and electrode is also very important. Compared with commercial electrode, Ag-RCM electrodes are softer and more biocompatible for long-term ECG monitoring. After the Ag-RCM electrode and commercial electrode were both worn for 5 h, the skin under the commercial electrode had a clear indentation (Fig. 7a), while the skin under the Ag-RCM electrode barely had any change (Fig. 7b). Examination of the impedance shows that the impedance of the Ag-RCM electrode after 5 h of wear (Fig. 7e) is almost no different from that of the unused Ag-RCM electrodes (Fig. 6a). And they do not become dehydrated and dry over time, as commercial electrodes do. Therefore, Ag-RCM electrodes can be used for long-term ECG monitoring. After they were rinsed with de-distilled water for 30 s and dried naturally, their impedance changed very little (Fig. 7f). In addition, after Ag-RCM electrodes were bent for 100 times, their resistance and conductivity (Fig. 7h) was tested. The results suggest that both of them change slightly and the variation is within 2 Ω and 20 s/cm respectively. As for the relatively large changes in resistance and conductivity for 0.15 and 0.20 mol/L Ag-RCM electrodes, they may be caused by the loss of a few Ag atoms after successive bending. Therefore, the Ag-RCM has good stability facing environmental changes as a good ECG electrode.

The Ag-RCM electrode was tested by XPS after being cleaned and worn. As can be found from Fig. 3d, the area of oxygen becomes larger after the Ag-RCM electrode was washed (Fig. 8d) and worn (Fig. 9d), which means that the content of oxygen on the surface of Ag-RCM increases due to the loss of Ag.

Performance of Ag-RCM electrodes in ECG monitoring

The Ag-RCM electrodes were designed as wristbands for long-term monitoring of ECG signals. The wrist strap was made up of two rectangular pieces of cotton cloth, Velcro straps and a Ag-RCM electrode.

A square pattern of 3*3 cm^2 was cut out with scissors on a long piece of cotton cloth with a width of 4 cm. The Ag-RCM was fixed to the blank space of the cotton cloth with glue and a buckle was fixed at the center of the Ag-RCM. Then the bottom and edges of the buckle were covered with cotton cloth so as to avoid interfering with the monitoring of the ECG signals. The upper surface of the Ag-RCM was covered with another piece of cotton cloth, which was sewn to the first piece (Fig. 10b). The ECG signals were monitored by a commercially available device BMD101 (Fig. 10b). In case of using commercial electrodes, the skin needs to be first rubbed with alcohol to reduce the resistance caused by the stratum corneum, while the prepared Ag-RCM electrodes can be used directly on the skin. The ECG signals of a volunteer, who has no history of heart disease, were monitored. Before monitoring, the volunteer was told to avoid unnecessary exercise and to sit still for 10 min to reduce the effect on the quality of the ECG signals. The electrode was put on the volunteer's wrist and connected to the BMD101 with a wire. The obtained ECG signals were transmitted via bluetooth (Fig. 10b) to the computer of the ECG monitoring device BMD101 and filtered using MATLAB2018. The ECG signals obtained by Ag-RCM electrodes prepared with different concentrations of $AgNO_3$ are all clear and stable (Fig. 10c ~ f). All P, Q, R, S and T waves are also clearly visible, and the monitored ECG signals contain much less noise than those of the commercial electrodes (Fig. 10g). However, as the concentration of $AgNO_3$ increases, the noise waves increase significantly, indicating that it is not that the more silver particles, the better. As the number of deposited silver particles increases, the network structures of the silver layer gradually decrease, reducing the performance of electron mobility. This indicates that the Ag-RCM electrode can replace the conventional Ag/AgCl electrodes.

Conclusions

In this work, we prepared a flexible dry electrode used in ECG sensor by electroless silver plating on a regenerated cellulose composite film. By controlling the amount of $AgNO_3$, the skin–electrode contact impedance of the Ag-RCM can be controlled. The ECG signals monitored by all the Ag-RCM electrodes are clearer and more stable than those of commercial Ag/AgCl electrodes. The skin–electrode contact impedance of the Ag-RCM electrode is similar to that of commercial Ag/AgCl electrode. The impedance of the Ag-RCM at 700 Hz is only 8 kΩ/cm^2, and the conductivity reaches 252 s/cm (when 0.20 mol/L $AgNO_3$ is used). After 5 h of wear, the skin contact impedance of the Ag-RCM electrode is only 10 kΩ/cm^2 (when 0.20 mol/L $AgNO_3$ is used). The maximum fluctuation range of the open circuit voltage of the Ag-RCM electrode is only 0.02 mv. In addition, the Ag-RCM electrode can fit the skin well without causing allergy. It is believed that the preparation of the Ag-RCM electrode can provide some new insights to the exploration of low-cost dry electrodes and monitoring devices.

Funding The authors have not disclosed any funding.

Declarations

Conflict of interest The authors declare that they have no known competing financial interests or personal relationships that could have appeared to influence the work reported in this paper.

References

Alawiye H, Kuhl E, Goriely A (2019) Revisiting the wrinkling of elastic bilayers I: linear analysis. Philos Trans A Math Phys Eng Sci 377:20180076. https://doi.org/10.1098/rsta.2018.0076

Beckmann L, Neuhaus C, Medrano G, Jungbecker N, Walter M, Gries T, Leonhardt S (2010) Characterization of textile electrodes and conductors using standardized measurement setups. Physiol Meas 31:233–247. https://doi.org/10.1088/0967-3334/31/2/009

Catrysse M, Puers R, Hertleer C, Van Langenhove L, van Egmond H, Matthys D (2004) Towards the integration of textile sensors in a wireless monitoring suit. Sens Actuators A 114:302–311. https://doi.org/10.1016/j.sna.2003.10.071

Chen Z, Li C, Ni Y, Kong F, Zhang Y, Kong A, Shan Y (2017) TCNQ-induced in-situ electrochemical deposition for the synthesis of silver nanodendrites as efficient bifunctional electrocatalysts. Electrochim Acta 239:45–55. https://doi.org/10.1016/j.electacta.2017.03.222

Ding ZD, Chi Z, Gu WX, Gu SM, Liu JH, Wang HJ (2012) Theoretical and experimental investigation on dissolution and regeneration of cellulose in ionic liquid. Carbohydr Polym 89:7–16. https://doi.org/10.1016/j.carbpol.2012.01.080

Huber T, Müssig J, Curnow O, Pang S, Bickerton S, Staiger MP (2011) A critical review of all-cellulose composites.

J Mater Sci 47:1171–1186. https://doi.org/10.1007/s10853-011-5774-3

Jayram ND, Aishwarya D, Sonia S, Mangalaraj D, Kumar PS, Rao GM (2016) Analysis on superhydrophobic silver decorated copper Oxide nanostructured thin films for SERS studies. J Colloid Interface Sci 477:209–219. https://doi.org/10.1016/j.jcis.2016.05.051

Jin J, Zheng D, Liu H (2017) The corrosion behavior and mechanical properties of CrN/Ni P multilayer coated mild steel as bipolar plates for proton exchange membrane fuel cells. Int J Hydrogen Energy 42:28883–28897. https://doi.org/10.1016/j.ijhydene.2017.10.046

Jo YJ et al (2020) Biocompatible and biodegradable organic transistors using a solid-state electrolyte incorporated with choline-based ionic liquid and polysaccharide. Adv Func Mater. https://doi.org/10.1002/adfm.201909707

Johar N, Ahmad I, Dufresne A (2012) Extraction, preparation and characterization of cellulose fibres and nanocrystals from rice husk. Ind Crops Prod 37:93–99. https://doi.org/10.1016/j.indcrop.2011.12.016

Kato M, Asoh TA, Uyama H (2019) Hydrogel adhesion by wrinkling films. Macromol Rapid Commun 40:e1900434. https://doi.org/10.1002/marc.201900434

Kuo C-H, Lee C-K (2009) Enhancement of enzymatic saccharification of cellulose by cellulose dissolution pretreatments. Carbohyd Polym 77:41–46. https://doi.org/10.1016/j.carbpol.2008.12.003

Lam K, McClelland S, Dallo MJ (2020) ECG: essential in care of patients with COVID-19. The Med J Aust. https://doi.org/10.5694/mja2.50841

Liu J et al (2020) Sacrificial layer-assisted one-step transfer printing for fabricating a three-layer dry electrode. Sens Actuators A Phys. https://doi.org/10.1016/j.sna.2020.111954

Ma B, Qiao X, Hou X, He C (2016) Fabrication of cellulose membrane with "imprinted morphology" and low crystallinity from spherulitic [Bmim]Cl. J Appl Polym Sci. https://doi.org/10.1002/app.43798

Ma B, Yang J, Sun Q, Jakpa W, Hou X, Yang Y (2017) Influence of cellulose/[Bmim]Cl solution on the properties of fabricated NIPS PVDF membranes. J Mater Sci 52:9946–9957. https://doi.org/10.1007/s10853-017-1150-2

Mackus AJ et al (2016) Atomic layer deposition of Pd and Pt nanoparticles for catalysis: on the mechanisms of nanoparticle formation. Nanotechnology 27:034001. https://doi.org/10.1088/0957-4484/27/3/034001

Nigusse AB, Malengier B, Mengistie DA, Tseghai GB, Van Langenhove L (2020) Development of washable silver printed textile electrodes for long-term ECG monitoring. Sensors (basel). https://doi.org/10.3390/s20216233

Oh SY, Yoo DI, Shin Y, Seo G (2005) FTIR analysis of cellulose treated with sodium hydroxide and carbon dioxide. Carbohydr Res 340:417–428. https://doi.org/10.1016/j.carres.2004.11.027

Pan Y, Wang W, Liu L, Ge H, Song L, Hu Y (2017) Influences of metal ions crosslinked alginate based coatings on thermal stability and fire resistance of cotton fabrics. Carbohydr Polym 170:133–139. https://doi.org/10.1016/j.carbpol.2017.04.065

Pei X, Li Y, Lu L, Jiao H, Gong W, Zhang L (2021) Highly dispersed Pd clusters anchored on nanoporous cellulose microspheres as a highly efficient catalyst for the Suzuki coupling reaction. ACS Appl Mater Interfaces 13:44418–44426. https://doi.org/10.1021/acsami.1c12850

Rosenau T, French AD (2021) N-Methylmorpholine-N-oxide (NMMO): hazards in practice and pitfalls in theory. Cellulose 28:5985–5990. https://doi.org/10.1007/s10570-021-03860-4

Sarafpour M, Youssefi M, Mortazavi SM (2017) Copper functionalization of polypropylene fabric surface in order to use in fog collectors. Fibers and Polymers 17:2041–2046. https://doi.org/10.1007/s12221-016-6560-2

Sun N, Rahman M, Qin Y, Maxim ML, Rodríguez H, Rogers RD (2009) Complete dissolution and partial delignification of wood in the ionic liquid 1-ethyl-3-methylimidazolium acetate. Green Chem. https://doi.org/10.1039/b822702k

Tan TH, Chang CS, Huang YF, Chen YF, Lee C (2011) Development of a portable Linux-based ECG measurement and monitoring system. J Med Syst 35:559–569. https://doi.org/10.1007/s10916-009-9392-4

Tasneem NT, Pullano SA, Critello CD, Fiorillo AS, Mahbub I (2020) A low-power on-chip ECG monitoring system based on MWCNT/PDMS dry electrodes. IEEE Sens J 20:12799–12806. https://doi.org/10.1109/jsen.2020.3001209

Todorov R, Lozanova V, Knotek P, Černošková E, Vlček M (2017) Microstructure and ellipsometric modelling of the optical properties of very thin silver films for application in plasmonics. Thin Solid Films 628:22–30. https://doi.org/10.1016/j.tsf.2017.03.009

Wang Y, Zhong X, Wang W, Yu D (2021) Flexible cellulose/polyvinyl alcohol/PEDOT:PSS electrodes for ECG monitoring. Cellulose 28:4913–4926. https://doi.org/10.1007/s10570-021-03818-6

Wu R et al (2019) A facile method to prepare a wearable pressure sensor based on fabric electrodes for human motion monitoring. Text Res J 89:5144–5152. https://doi.org/10.1177/0040517519849451

Xu X, Luo M, He P, Guo X, Yang J (2019) Screen printed graphene electrodes on textile for wearable electrocardiogram monitoring. Appl Phys A. https://doi.org/10.1007/s00339-019-3006-x

Yao Y et al (2016) Interfacial engineering of silicon carbide nanowire/cellulose microcrystal paper toward high thermal conductivity. ACS Appl Mater Interfaces 8:31248–31255. https://doi.org/10.1021/acsami.6b10935

Ye W, Li Y, Yang B, Wang C (2007) Comparative study of electrolessly deposited Pd/Ag films onto p-silicon (100)-activated seed layers of Ag and Pd. J Solid State Electrochem 11:1347–1351. https://doi.org/10.1007/s10008-007-0298-0

Yoon Y, Cho JH, Yoon G (2009) Non-constrained blood pressure monitoring using ECG and PPG for personal healthcare. J Med Syst 33:261–266. https://doi.org/10.1007/s10916-008-9186-0

Yu X, Bao X, Zhou C, Zhang L, Yagoub AEA, Yang H, Ma H (2018) Ultrasound-ionic liquid enhanced enzymatic and acid hydrolysis of biomass cellulose. Ultrason Sonochem

41:410–418. https://doi.org/10.1016/j.ultsonch.2017.09.003

Zhao H, Baker GA, Song Z, Olubajo O, Crittle T, Peters D (2008) Designing enzyme-compatible ionic liquids that can dissolve carbohydrates. Green Chem. https://doi.org/10.1039/b801489b

Zhao H, Kwak J, Wang Y, Franz J, White J, Holladay J (2007) Interactions between cellulose and N-Methylmorpholine-N-Oxide. Carbohydr Polym 67:97–103. https://doi.org/10.1016/j.carbpol.2006.04.019

Zhou Y, Ding X, Zhang J, Duan Y, Hu J, Yang X (2014) Fabrication of conductive fabric as textile electrode for ECG monitoring. Fibers Polym 15:2260–2264. https://doi.org/10.1007/s12221-014-2260-y